Engineering with Computers (2021) 37:1409–1428
https://doi.org/10.1007/s00366-019-00892-0

ORIGINAL ARTICLE

On the application of Harris hawks optimization (HHO) algorithm to the design of microchannel heat sinks

Ahmad Abbasi[1] · **Behnam Firouzi**[1] · **Polat Sendur**[1]

Received: 19 August 2019 / Accepted: 22 November 2019 / Published online: 3 December 2019
© Springer-Verlag London Ltd., part of Springer Nature 2019

Abstract

A novel Harris hawks optimization algorithm is applied to microchannel heat sinks for the minimization of entropy generation. In the formulation of the heat transfer model of the microchannel, the slip flow velocity and temperature jump boundary conditions have been taken into account. A variety of materials and fluids have also been evaluated to determine the optimal design of the microchannel. Since the main objective of this paper is to assess the search and exploration ability of the novel Harris Hawks algorithm, results are also benchmarked with those of commonly used particle swarm optimization, bees optimization algorithm, grasshopper optimization algorithm, whale optimization algorithm and dragonfly algorithm. Finally, results are compared to the analytical results and results obtained by the application of genetic algorithms. Results show that the Harris hawks algorithm has a superior performance in minimizing the entropy generation of the microchannel. The algorithm is also more computationally efficient compared to the aforementioned algorithms. Moreover, optimization results indicate that the use of copper for the microchannel and ammonia as the coolant leads to minimal entropy generation and, therefore, is considered as the best design. Considering the poor corrosive characteristics of copper, aluminum as the microchannel material is proposed as an alternative.

Keywords Optimization · Harris hawks optimization (HHO) · Entropy generation · Micro-channel heat sink · Knudsen number · Metaheuristic optimization

List of symbols

A	Surface area of heating (mm^2)
C_p	Specific heat of fluid (J kg^{-1} K^{-1})
D_h	Hydraulic diameter (mm)
f	Friction factor
G	Volume flow rate (m^3 s^{-1})
H_c	Channel height (mm)
h_av	Average heat transfer coefficient (W m^{-2} K^{-1})
h_fin	Heat transfer coefficient for base surface (W m^{-2} K^{-1})
h_base	Heat Transfer coefficient along fin surface (W m^{-2} K^{-1})
Kn	Knudsen number
K	Thermal conductivity of solid (W m^{-1} K^{-1})
K_a	Thermal conductivity of air (W m^{-1} K^{-1})
k_ce	Sum of entrance and exit losses
k_eq	Ratio of thermal conductivity of fluid to solid
K_s	Slip constant
L	Length of channel in flow direction (mm)
m	Fin parameter (m^{-1})
$\dot{m}$	Total mass flow rate (kg s^{-1}) (the same symbol is used for fin parameter ABOVE)
N	Total number of microchannels
Nu_Dh	Nusselt number based on hydraulic diameter
Pe_Dh	Peclet number based on hydraulic diameter
Pr	Prandtl number
q	Heat flux (W m^{-2})
R	Resistance (K W^{-1})
Re_Dh	Reynolds number based on hydraulic diameter
S_gen	Total entropy generation rate (W K^{-1})
T	Absolute temperature (K)
U_av	Average velocity in channels (m s^{-1})
U_s	Slip velocity (m s^{-1})
W	Width of heat sink (mm)
W_c	Half of the channel width (mm)

✉ Behnam Firouzi
behnam.firoozi@ozu.edu.tr

Ahmad Abbasi
ahmad.abbasi@ozu.edu.tr

Polat Sendur
polat.sendur@ozyegin.edu.tr

[1] Mechanical Engineering Department, Ozyegin University, Istanbul, Turkey

Greek symbols

α	Thermal diffusivity ($m^2\ s^{-1}$)
α_c	Channel aspect ratio
α_{hs}	Heat sink aspect ratio
β	Fin spacing ratio
ΔP	Pressure drop across microchannel (Pa)
η_{fin}	Fin efficiency
γ	Ratio of specific heats
λ	Mean free path (m)
μ	Absolute viscosity of fluid ($kg\ m^{-1}\ s^{-1}$)
ν	Kinematic viscosity of fluid ($m^2\ s^{-1}$)
ρ	Fluid density ($kg\ m^{-3}$)
σ	Tangential momentum accommodation coefficient
σ_t	Energy accommodation coefficient
ζ_u	Slip velocity coefficient
ζ_t	Temperature jump coefficient

Subscripts

a	Ambient
av	Average
b	Base surface
c	Channel
ce	Contraction and expansion
conv	Convective
f	Fluid
fin	Single fin
h	Hydraulic
hs	Heat sink
in	Inlet
out	Outlet
s	Slip
th	Thermal
w	Wall

1 Introduction

Thermal management of electronic devices has become increasingly important for the design of products with increased power and efficiency in the electronics industry. Hence, for higher heat dissipation, lower coolant requirement and many other advantages due to the small size, microchannel heat sinks were first introduced by Tuckerman and Pease [1]. Nowadays, they are used as one of the most common methods of removing heat from electronics devices. In these devices, the heat transfer coefficient is inversely proportional to the channel hydraulic diameter [2].

One common way to improve the performance of engineering structures and design is using meta-heuristic algorithms in the optimization field. Many meta-heuristic algorithms have been introduced in the evolutionary computation and optimization field in recent years. For example, the particle swarm optimization (PSO) [3] algorithm has been inspired from the bird migration, and the imperialist competitive algorithm (ICA) [4] from social and human relationships to develop mathematical models and related optimization algorithms. The optimization problem has a direct relationship with the search, and its relevance is inspired by nature, for example, in the ant colony optimization (ACO) algorithm [5], the ants always look for the best food source and its saving. In the artificial bee colony (ABC) algorithm [6], the bees look for the best flower for honey production. Furthermore, several swarm intelligence algorithms have been recently developed. For example, grasshopper optimization algorithm (GOA) mimics the swarming behavior of grasshoppers in nature [7]. Similarly, dragonfly algorithm (DA) [8] and whale optimization algorithm (WOA) [9] are inspired from the behavior of dragonflies and whales, respectively. There is a vast body of literature on the successful applications of nature-inspired algorithms for solving different engineering problems [10–16]. Nature seeks to make the most resistant and superior creatures. Solvers capability of finding the best solution amongst the infinite solutions is critical for efficiently solving optimization problems. In fact, searching and optimization are applied to these problems, and those algorithms are more applicable here which investigate a large part of the solutions and arrive at a final solution.

In all conventional optimization methods, there are two phases in the common search phase: (a) exploration and (b) exploitation. The exploration ability aims at generating new and varied responses, while the exploitation ability is mainly responsible for the local improvement of the responses from the exploration phase. An efficient algorithm is considered as the one, which provides a balance between the two components [17].

HHO is a novel optimization method developed by Heidari et al. [18], which is inspired from the modeling of the behavior of Harris Hawks. Attacking strategy of Harris Hawks simultaneously from various directions has been the building block of the algorithm. This algorithm has shown high search power, acceptable exploitation and exploration, which led to their successful application to many real engineering problems compared to previous algorithms [19–27]. In HHO algorithm, firstly, eagles (search agents) try to search in the solution space effectively, thereby gathering information about the solution space. This information is then used by HHO algorithm to avoid being trapped to local optimums. After a comprehensive search, by using a group attack, hawks try to find the best solution region. Another key factor that leads to the superiority of this algorithm is the fact that HHO algorithm is able to update the search agents, which eventually lead to finding the global optimum. Applicability of this algorithm to the applications with many variables also make this algorithm an attractive alternative. On the other hand, other algorithms are, in general, accurate for one or two-dimensional problems. HHO algorithm is applicable to higher-dimensional problems by balancing exploration and exploitation phases [7].

Moayedi et al. [19] used HHO and DA optimization methods to analyze the bearing capacity of footing over two-layer foundation soils. In another work, they studied the effect of HHO optimization algorithm to enhance the accuracy of the conventional multilayer perception technique to find a more reliable analysis of the stability of the soil slobes [20]. Abdel Aleem et al. [21] optimized the harmonic overloading level of frequency-dependent components in a non-sinusoidal distribution system using HHO algorithm. They have proven that HHO is an effective algorithm compared to other algorithms. Yildiz et al. [22] studied the performance of HHO, GOA, MVO for solving manufacturing optimization problems. They showed that these algorithms are powerful for the manufacturing applications. Furthermore, the results of this study demonstrate that HHO is able to find the optimal solution with lower number of function evaluations. HHO algorithm was also used in the literature to find the optimal tuning of convolutional neural network parameters for the control chart patterns recognition [23]. Moreover, Mehta et al. [24] showed that HHO algorithm can be considered as an efficient optimization algorithm for solving the optimum load dispatch problems.

While HHO algorithm has shown a great performance in so many engineering problems, No Free Lunch (NFL) theorem states that none of the metaheuristic algorithms result in the best solutions for all problems. Therefore, it is required to calibrate optimization parameters to improve their performance. One of the limitations of HHO is that it cannot be used directly for binary problems. Too et al. [28] proposed a binary version of HHO making it possible for its application to the binary problems such as feature selection problems. This has been achieved by integrating S-shaped and V-shaped transfer functions to the HHO algorithm. Hussain et al. [29] modified the HHO algorithm with a long-term memory concept to apply it to higher dimensional and optimal power flow problems. Chen et al. [30] added one more exploration mechanism to the HHO algorithm to identify the unknown parameters of photovoltaic modulus efficiently. In this study, they used opposition-based learning and chaotic local search simultaneously to enhance its diversification algorithm. Jia et al. [31] used a dynamic control parameter method and mutation operator to modify the HHO and apply it for the satellite Image Segmentation. They concluded that the exploration and exploitation phases are not balanced, and this algorithm may not be able to yield global optimum for some complex problems. It is shown that this modification improves the search capability of the HHO, thereby leading to global optimum compared to original HHO algorithm. A new hybrid algorithm, which combines Harris Hawk algorithm and Nelder-Mead, is used by Yildiz et al. [32] for the optimization of process parameters of milling operations. Furthermore, Bao et al. [33] added differential evolution (DE) algorithm to the HHO algorithm for solving color image multilevel thresholding segmentation problems. In this paper, both algorithms of HHO and DE work at the same time to update the positions of each sub-population more efficiently. This study concludes that HHO-DE algorithm has superior performance for multi-level thresholding color image segmentation. In another study, Bui et al. [34] combined the Harris Hawk optimization (HHO) with artificial neutral network (ANN) for improving the ability of original HHO in landslide susceptibility analysis.

Application of the optimization methods to MEMS electronics for the effective cooling by microchannel heat sinks have become popular in the recent years for the aforementioned reasons. In one of those studies, Wang et al. [35] optimized the geometric design of microchannel heat sink using the multi-parameter optimization methods. In this study, design parameters such as the number of channels, channel width, and channel height were optimized so as to minimize the heat transfer resistance. In another study by Bello-Ochende et al. [36], minimization of the peak temperature from microchannel heat sink walls was chosen as the objective function using the finite volume method. In a more recent study, Cruz-Duarte [37] developed an optimal microchannel heat sinks design with colloidal coolants by minimizing entropy generation. In this process, three optimization algorithms including unified Particle swarm optimization, spiral optimization and cuckoo were used and their performance was compared. They showed that the cuckoo algorithm provides a more accurate response than the other two methods. In another paper [38], using optimization methods such as SA, SO and UPSO, they investigated the minimization of heat resistance in micro channel heat sinks with spreading resistance.

Adham et al. [39] analyzed methods to improve micro channel heat sink performance by combining the classic optimization of genetic algorithm with EGM. In this process, the genetic algorithm has been used with different methodologies to improve optimization.

There is a vast body of literature on the minimization of the thermal resistance of microchannel heat sinks. Afzal Hussain and Kim [40] minimized the thermal resistance in a microchannel by optimizing the width and depth of the microchannel and fin width. In another study [41], they attempted to optimize the performance of microchannel heat sinks using hybrid multi-objective evolutionary algorithm coupled with surrogate methods, where multi-objectives were chosen as the thermal resistance and pumping power.

Furthermore, the effectiveness of different algorithms on the performance of microchannels has been compared in various works. Most common algorithms from the literature are MOGA [42], MOEA [43], prey-predator algorithm and Artificial Neutral network [44] GA and Taguchi methods [45] and Ant Lion algorithm [46]. Khan et al. [28] minimized the entropy generation rate in microchannel heat sinks using Genetic Algorithms. In this study, the optimization results were compared with those obtained from the Newton–Raphson method.

Given the articles cited in the literature review, improving the performance of micro channel heat sinks by optimizing the design of these structures is an important topic with high importance in the electrical equipment and MEMS industries. Among the previous studies, many researchers have tried to improve the performance of thermal microchannels using optimization algorithms [35–47]. Among them, only in one study conducted by Khan et al. [28], the slip flow velocity and temperature jump boundary conditions have been considered in calculating friction and heat transfer coefficient. It is noteworthy that in Khan's study [47], the classical genetic optimization algorithm has been used. In this study, by using a new swarm intelligence algorithm called HHO (introduced in 2019), the most optimal possible solution and design parameters were obtained by considering the slip flow, and its performance has been compared to the results of the aforementioned algorithms such as bees algorithm (BeA), grasshopper optimization algorithm (GOA), whale optimization algorithm(WOA), dragonfly algorithm (DA) and particle swarm optimization (PSO) algorithms. In addition, results are considered for different fluids and microchannel materials to achieve the best performance. The organization of the paper is as follows: first, modeling of the heat transfer problem is explained in Sect. 2. An overview of the HHO optimization algorithm is given in Sect. 3. In Sect. 4, optimization methodology is explained in detail. The results are presented in Sect. 5. Finally, conclusions are addressed in Sect. 6.

2 Modeling

The geometry of the microchannel heat sink is shown in Fig. 1. It consists of N parallel microchannels with a rectangular cross-section ($2W_c \times H_c$), length and width are respectively equal to L and W (Fig. 1). It is noteworthy to be mentioned that the upper surface of micro-channel is isolated, and the bottom surface of it is uniformly heated. The thickness of the fin and temperature of the internal wall are $2W_w$ and T_w, respectively. Heat is dissipated away by a fluid as a coolant with the temperature of T_a and the velocity of U_{av}. For calculation of friction and heat transfer coefficient in channel's wall, Slip flow velocity, and temperature jump boundary conditions are taken into account.

Half of the channel is considered for the analysis of the performance of the microchannel heat sink as shown in Fig. 1. The side and the top surfaces can be considered impenetrable, adiabatic and shear free i.e. no mass and shear work transfer across these surfaces. The system's irreversibility is due to heat transfer and friction. For convenience, the following assumptions are taken into account:

Fig. 1 The geometry of the microchannel heat sink

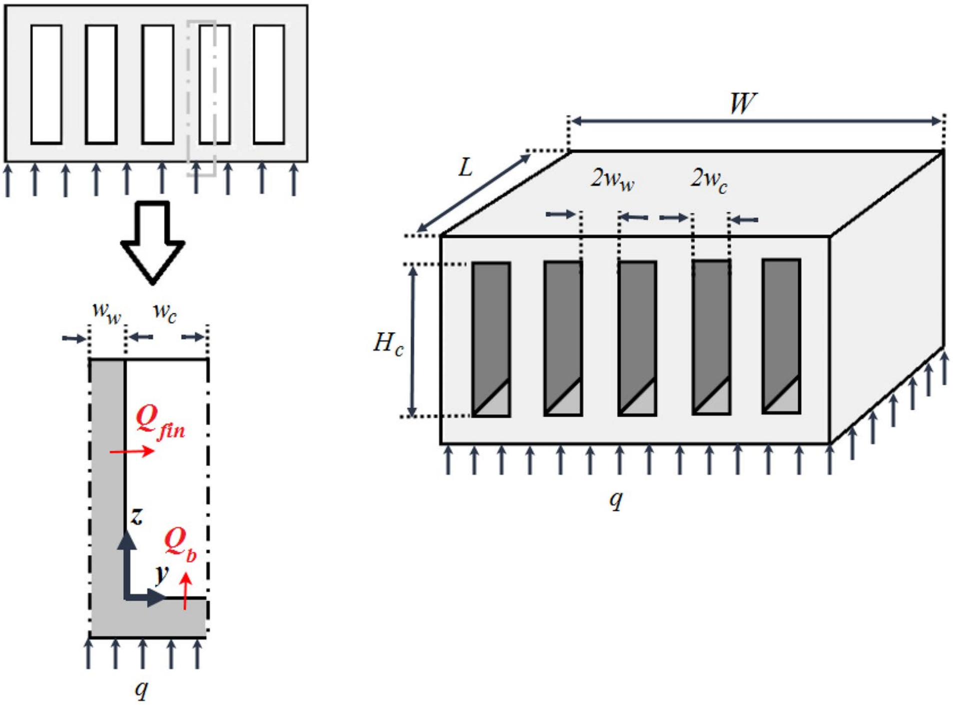

- The fluid is compressible with constant thermodynamic properties.
- The fluid flow is fully developed fluid flow.
- The fluid flow is 2D and steady-state laminar.
- The material for the microchannels is isotropic.
- The surfaces of the wall of microchannels are smooth.
- There is uniform heat flux from the bottom surface of the microchannel.
- Adiabatic fin tips boundary conditions are assumed.
- Slip flow (which is between 0.1 and 0.001) without considering creep effect.
- The change in kinetic and potential energies is negligible.

2.1 Entropy generation formulation

The conservation of mass equation for specified control volume (see Fig. 1) is defined as follows:

$$\frac{\mathrm{d}m_{\mathrm{cv}}}{\mathrm{d}t}=\dot{m}_{\mathrm{in}}-\dot{m}_{\mathrm{out}} \tag{1}$$

where $\dot{m}_{\mathrm{in}}$ and $\dot{m}_{\mathrm{out}}$ are the mass rate at the inlet and outlet of the microchannel, respectively. $\frac{\mathrm{d}m_{\mathrm{cv}}}{\mathrm{d}t}$ is the mass rate of the control volume. Equation (1) is re-written as follows with the steady state assumption:

$$\dot{m}_{\mathrm{in}}=\dot{m}_{\mathrm{out}}=\dot{m} \tag{2}$$

The application of the first law of thermodynamics to the aforementioned control volume in steady-state condition and neglecting kinetic and potential energies results in:

$$Q=\dot{m}\left(h_{\mathrm{out}}-h_{\mathrm{in}}\right) \tag{3}$$

where Q is the total heat transfer from the fin and base of the microchannel. $h_{\mathrm{in}}, h_{\mathrm{out}}$ are the inlet and outlet enthalpies of the fluids, respectively. Equation 4 is obtained by the application of the second law of thermodynamics according to the procedure from [48, 49]:

$$\frac{\mathrm{d}S_{\mathrm{cv}}}{\mathrm{d}t}=\dot{m}\left(s_{\mathrm{in}}-s_{\mathrm{out}}\right)+\frac{Q_{\mathrm{fin}}}{T_{\mathrm{a}}}+\frac{Q_{\mathrm{b}}}{T_{\mathrm{b}}}+S_{\mathrm{gen}} \tag{4}$$

where $\frac{\mathrm{d}S_{\mathrm{cv}}}{\mathrm{d}t}$ is the entropy rate of the control volume. T_{b} and Q_{b} are the temperature and heat transfer of the base of heat sink, Q_{fin} is the heat transfer from the fin and S_{gen} is the entropy generation. $s_{\mathrm{in}}, s_{\mathrm{out}}$ are the inlet and outlet entropies of the fluids. The left hand's side of Eq. 4 becomes zero under the steady-state condition. In addition, the heat transfer from the fin and base add to the total heat transfer resulting in:

$$S_{\mathrm{gen}}=\dot{m}\left(s_{\mathrm{out}}-s_{\mathrm{in}}\right)-\frac{Q}{T_{\mathrm{b}}} \tag{5}$$

By integrating Gibb's equation one can find:

$$h_{\mathrm{in}}-h_{\mathrm{out}}=T_{a}\left(s_{\mathrm{in}}-s_{\mathrm{out}}\right)+\frac{1}{\rho}\left(P_{\mathrm{in}}-P_{\mathrm{out}}\right) \tag{6}$$

where ρ is the density of the fluid. $P_{\mathrm{in}}, P_{\mathrm{out}}$ are the inlet and outlet pressure of the fluids, respectively. By substituting Eqs. (3) and (5) into Eq. (6) and considering $\theta_{\mathrm{b}}=T_{\mathrm{b}}-T_{\mathrm{a}}$, we have:

$$S_{\mathrm{gen}}=\frac{Q\theta_{\mathrm{b}}}{T_{\mathrm{a}}T_{\mathrm{b}}}+\frac{\dot{m}}{\rho T_{\mathrm{b}}}\Delta P \tag{7}$$

where P is the total pressure drop across the microchannel and $\theta_{\mathrm{b}}=R_{\mathrm{th}}Q$. So, the final form of Eq. (7) becomes as:

$$S_{\mathrm{gen}}=\frac{Q^{2}R_{\mathrm{th}}}{T_{\mathrm{a}}T_{\mathrm{b}}}+\frac{\dot{m}}{\rho T_{\mathrm{b}}}\Delta P \tag{8}$$

where R_{th} is total thermal resistance across the microchannel. The expression in Eq. 8 is the entropy generation equation, which consists of thermal resistance and pressure drop.

The number of channels for the specified dimensions is calculated as follows:

$$N=\frac{W-w_{\mathrm{w}}}{w_{\mathrm{c}}-w_{\mathrm{w}}} \tag{9}$$

w_{w} is half of the width of the channel and w_{c} is the half of the fin of the microchannel. Given the total flow rate, height and width of the microchannel, the average velocity in each channel can be obtained from Eq. (10):

$$U_{\mathrm{av}}=\frac{\dot{m}}{N\rho(2w_{\mathrm{w}})H_{\mathrm{c}}} \tag{10}$$

where H_{c} is the height of microchannel.

2.2 Thermal resistance of microchannel

Thermal resistance taking into account the convective and fluid thermal resistances is calculated from:

$$\begin{aligned}R_{\mathrm{th}}&=\frac{\theta_{\mathrm{b}}}{Q}\\R_{\mathrm{th}}&=\frac{T_{\mathrm{b}}-T_{\mathrm{f}}}{Q}+\frac{T_{\mathrm{f}}-T_{\mathrm{a}}}{Q}\\R_{\mathrm{th}}&=R_{\mathrm{conv}}+R_{\mathrm{fluid}}\end{aligned} \tag{11}$$

where T_{f} is the bulk fluid temperature. The temperature of base surface of microchannel and bulk fluid can be written calculated according to Eqs. (12) and (13), respectively:

$$T_{\mathrm{b}}=T_{\mathrm{a}}+QR_{\mathrm{th}} \tag{12}$$

$$T_{\mathrm{f}} = T_{\mathrm{a}} + \frac{Q}{2C_p\dot{m}} \tag{13}$$

where C_p is the specific heat of fluid. Assuming same heat transfer coefficient for fin and base, i.e. ($\mathrm{h_{base}} = \mathrm{h_{fin}} = \mathrm{h_{av}}$), the thermal resistance reduces to:

$$R_{\mathrm{conv}} = \frac{1}{Ah_{\mathrm{av}}} \tag{14}$$

$$R_{\mathrm{fluid}} = \frac{1}{C_p\dot{m}} \tag{15}$$

where h_{av} is the average heat transfer coefficient. A is the contact surface, which can be calculated from Eq. (16):

$$A = 2NL(W_{\mathrm{c}} + H_{\mathrm{c}}\eta_{\mathrm{fin}}) \tag{16}$$

Fin efficiency (η_{fin}) is defined as follow [50]:

$$\eta_{\mathrm{fin}} = \frac{\tanh\left(mH_{\mathrm{c}}\right)}{mH_{\mathrm{c}}} \tag{17}$$

$$m = \sqrt{\frac{2h_{\mathrm{av}}}{kw_{\mathrm{c}}}} \tag{18}$$

where m is the fin parameter and k is the thermal conductivity of the fin. Khan et al. [49] determined the Nusselt number in the dimensionless form by solving energy equation and taking into account the slip flow velocity and temperature boundary conditions:

$$\mathrm{Nu} = \frac{h_{\mathrm{av}}D_{\mathrm{h}}}{k_{\mathrm{f}}} \tag{19}$$

$$\mathrm{Nu} = \frac{140/17}{\left(1+\alpha_{\mathrm{c}}\right)\left[1 - \frac{6}{17}\frac{U_{\mathrm{s}}}{U_{\mathrm{av}}} + \frac{2}{51}\left(\frac{U_{\mathrm{s}}}{U_{\mathrm{av}}}\right)^2\right] + \frac{140}{17}\xi_t} \tag{20}$$

$$\alpha_{\mathrm{c}} = \frac{2w_{\mathrm{c}}}{H_{\mathrm{c}}} \tag{21}$$

$$\frac{U_{\mathrm{s}}}{U_{\mathrm{av}}} = \frac{6\alpha}{1+6\alpha} \tag{22}$$

$$\alpha = \frac{2\xi_u}{1+\alpha_{\mathrm{c}}} \tag{23}$$

$$\xi_u = \left(\frac{2-\sigma}{\sigma}\right)\mathrm{Kn} \tag{24}$$

$$\xi_t = \left(\frac{2-\sigma_{\mathrm{t}}}{\sigma_{\mathrm{t}}}\right).\frac{2\gamma}{\gamma+1}.\frac{\mathrm{Kn}}{\mathrm{Pr}} \tag{25}$$

where D_{h} is the hydraulic diameter and k_{f} is the thermal conductivity of the fluid, U_{s} is the slip velocity of the fluid, α is the thermal diffusivity, ξ_u is the slip velocity coefficient,ξ_t is the temperature jump coefficient, σ_t is the energy accommodation coefficient, Pr Prandtl number, γ is the ratio of specific heat. Kn is the Knudsen number, which characterizes the boundary condition of the fluid.

By using the above equations thermal resistance can be calculated according to Eqs. (26) to (31):

$$R_{\mathrm{th}} = \frac{2C_3\alpha_{\mathrm{hs}}}{LC_1C_2k_{\mathrm{f}}} \tag{26}$$

$$C_1 = N\alpha_{\mathrm{hs}}\left(2\eta_{\mathrm{fin}} + \alpha_{\mathrm{c}}\right) \tag{27}$$

$$C_2 = \left(1+\alpha_{\mathrm{c}}\right)/\alpha_{\mathrm{c}} \tag{28}$$

$$C_3 = \frac{1}{\mathrm{Nu_{Dh}}} + \frac{C_1}{\mathrm{Pe_{Dh}}} \tag{29}$$

$$\alpha_{\mathrm{hs}} = \frac{L}{2w_{\mathrm{c}}} \tag{30}$$

$$\beta = \frac{w_{\mathrm{c}}}{w_{\mathrm{w}}} \tag{31}$$

2.3 Pressure drop formulation

Pressure drop due to flow across the channel is as follow:

$$\Delta P = \frac{\rho U_{\mathrm{av}}^2}{2}\left[K_{\mathrm{ce}} + \left(f\frac{L}{D_{\mathrm{h}}}\right)\right] \tag{32}$$

where K_{ce} is the sum of entrance and exit losses. Khan et al. [48] calculated the friction coefficient of a rectangular microchannel in terms of aspect ratio and slip velocity coefficient as:

$$f\mathrm{Re_{Dh}} = \left(\frac{24}{1+\alpha_{\mathrm{c}}}\right).\left(\frac{1}{1+6\alpha}\right) \tag{33}$$

where $\mathrm{Re_{Dh}}$ is the Reynold's number and f is the friction factor. K_{ce} can be expressed as follow [51, 52]:

$$K_{\mathrm{ce}} = 1.79 - 2.32\left(\frac{w_{\mathrm{c}}}{w_{\mathrm{c}}+w_{\mathrm{w}}}\right) + 0.53\left(\frac{w_{\mathrm{c}}}{w_{\mathrm{c}}+w_{\mathrm{w}}}\right)^2 \tag{34}$$

By substituting the above equation in the Eq. (8) S_{gen} can be found as follow:

$$S_{\mathrm{gen}} = \frac{Q^2}{T_{\mathrm{a}}T_{\mathrm{b}}} \cdot \frac{2C_3\alpha_{\mathrm{hs}}}{LC_1C_2k_{\mathrm{f}}} + \frac{\rho w_{\mathrm{c}} H_{\mathrm{c}} U_{\mathrm{av}}^3}{T_{\mathrm{a}}} C_4 \tag{35}$$

$$C_4 = \left[K_{\mathrm{ce}} + \left(f\frac{L}{D_{\mathrm{h}}}\right)\right] \tag{36}$$

3 HHO optimization algorithm

HHO is a novel optimization method developed by Heidari et al. [18]. HHO is a nature-inspired optimization algorithm inspired by the Harris Hawk birds' behavior modeling. The essence of the algorithm is the cooperation between hawks in hunting the prey. Based on this algorithm, a group of Harris hawks attack the prey from different directions to take it by surprise. Evidently, the prey's escape pattern is proportional to the Harris hawk's chase model. Birds cooperate in the process of attack. Meanwhile, the leader of the Harris hawks attacks the target prey, follows it, and suddenly moves out of sight, and the next Harris hawk continues the chase. This strategy tires the prey and eventually results in its capture. HHO algorithm is more superior to other algorithms on its applicability to constrainted problems. Moreover, HHO, which is a global optimizer, can maintain its balance between exploitation and exploration phases. The HHO algorithm has three phases. The first phase is the ability of exploration, which is formulated as follows:

$$x(t+1) = \begin{cases} x_{\mathrm{rand}}(t) - r_1\left|x_{\mathrm{rand}}(t) - 2r_2x(tt\right| & q \geq 0.5 \\ x_{\mathrm{prey}}(t) - x_a(t) - r_3(LB + r_4(UB - LB)) & q < 0.5 \end{cases} \tag{37}$$

where $X(t)$ is the current location of Hawk, $X(t+1)$ is the location of Hawk in the next iteration t, $X_{\mathrm{prey}}(t)$ is the location of prey, r_1, r_2, r_3, r_4 and q are random numbers between (0,1). $X_{\mathrm{rand}}(t)$ is the randomly selected hawk between the population. Furthermore, LB and UB denote the lower bands and the upper bands, respectively. $X_{\mathrm{a}}(t)$ is the average location of Harris Hawk, which is given as below:

$$x_{\mathrm{a}}(t) = \frac{1}{N}\sum_{i=1}^{N} x_i(t) \tag{38}$$

where $X_i(t)$ demonstrates the position of each Harris Hawk in iteration t and N is the number of all Harris Hawks. The second phase is the exploitation. Evidently, the hawks' energy is reduced during chase and hunt. The energy of a prey can be defined as:

$$E = 2E_0\left(1 - \frac{1}{T}\right) \tag{39}$$

E_0 is the energy in the first stage, T indicates the maximum number of iterations and E is the escaping energy. In this phase, when $\left|E_0\right| \geq 1$ exploration happens and when $\left|E_0\right| < 1$ exploitation occurs.

The third phase is exploitation, which is mainly to improve the local solutions from previously found solutions. This phase is the hawks' surprising attack on the prey identified in the previous phase. Based on the prey's escape and hawks' chasing, four models have been proposed for the attack phase. Different phases of the HHO algorithm are shown in Fig. 2.

3.1 Soft besiege

Soft besiege condition is valid when $r \geq 0$ and $|E| \geq 0$, which is modeled as:

$$x(t+1) = \Delta x(t) - E\left|Jx_{\mathrm{prey}}(t) - 2x(t)\right| \tag{40}$$

$$\Delta x(t) = x_{\mathrm{prey}}(t) - x(t) \tag{41}$$

where Δx is the difference between the prey location and the current location of Hawk in the iteration t. J is the random jump power of the prey while it is escaping which is equal to $J = 2(1 - r_5)$ and r_5 is a random number in the interval (0,1).

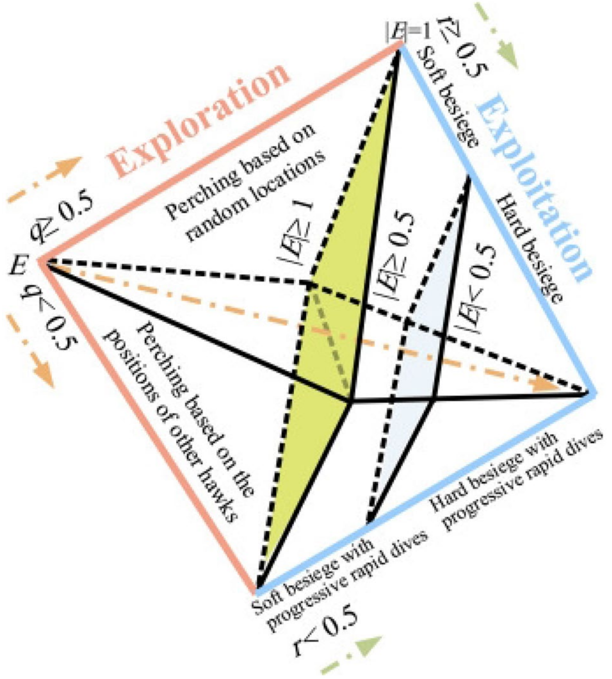
|E|=1
r≥0.5
Soft besiege
Exploitation
Hard besiege
Exploration
Perching based on random locations
q≥0.5
E
q<0.5
|E|≥1
|E|≥0.5
|E|<0.5
Perching based on the positions of other hawks
Hard besiege with progressive rapid dives
Soft besiege with progressive rapid dives
r<0.5

Fig. 2 Different phases of HHO algorithm [18]

3.2 Hard besiege

Hard besiege condition is valid when $r \geq 0$ and $|E| \prec 0$. The prey is tired and does not have sufficient energy to escape. This phase is modeled as follows:

$$x(t+1) = x_{\text{prey}}(t) - E_n|\Delta x(t)| \tag{42}$$

3.3 Soft besiege with progressive rapid dive

Soft besiege with progressive rapid dive condition is valid when $r \prec 0$ and $|E| \geq 0$. In this phase, the prey has enough energy to escape successfully. In this stage, for performing soft besiege Hawk examines the next move that can be formulated as follows:

$$x = x_{\text{prey}}(t) - E\left|Jx_{\text{prey}}(t) - x(t)\right| \tag{43}$$

$$Z = Y + S + \text{LF}(D) \tag{44}$$

where D indicates the dimension and S is a random vector by size $1 \times D$ and LF is the levy flight function [18, 53]. As a result we have:

$$x(t+1) = \begin{cases} Y & f(Y) \prec f(y(t)) \\ Z & f(Z) \prec f(y(t)) \end{cases} \tag{45}$$

1. Hard besiege with progressive rapid dive
2. Hard besiege with progressive rapid dive is valid when $r \prec 0$ and $|E| \prec 0$. In this case, the prey does not have enough energy to escape appropriately. This strategy can be formulated as follows:

$$x(t+1) = \begin{cases} x_{\text{prey}}(t) - E\left|Jx_{\text{prey}}(t) - x_m(t)\right| & f(Y) \prec f(y(t)) \\ Z = Y + S + \text{LF}(D) & f(Z) \prec f(y(t)) \end{cases} \tag{46}$$

4 Optimization methodology

The objective function is defined as the minimization of the entropy generation. The constraints are put for the geometric dimensions of the microchannel. The optimization problem is formulated in Eq. (47) with the objective function and constraints in the negative null form:

$$F(x) = S_{\text{gen}} = \frac{Q^2}{T_{\text{a}}T_{\text{b}}}\cdot\frac{2C_3\alpha_{\text{hs}}}{LC_1C_2k_{\text{f}}} + \frac{\rho w_{\text{c}}H_{\text{c}}U_{\text{av}}^3}{T_{\text{a}}}C_4 \tag{47}$$

$$\begin{aligned} \text{Subject to}: 0.1 &< 2W_{\text{c}} < 0.3 \\ 0.1 &< 2W_{\text{w}} < 0.3 \\ 3 &< H_{\text{c}} < 8 \end{aligned} \tag{48}$$

For the optimization case study, silicon and air are chosen as the material for the microchannel and the coolant, respectively. Harris Hawk's optimization algorithm (HHO) is applied to obtain the optimal design variables in terms of two dimensionless parameters: channel aspect ratio ($\alpha_{\text{c}} = \frac{2W_{\text{c}}}{H_{\text{c}}}$) and fin spacing ratio ($\beta = \frac{W_{\text{c}}}{W_{\text{w}}}$). Fin spacing ratio is related to the width of channels and thickness of fin. Furthermore, the channel aspect ratio depends on the width and height of channels. HHO algorithm for the optimization of microchannel heat sink (MCHS) is shown in Fig. 3. The recommended parameters from the literature are used for PSO, BeA, GOA, WOA, DA and HHO

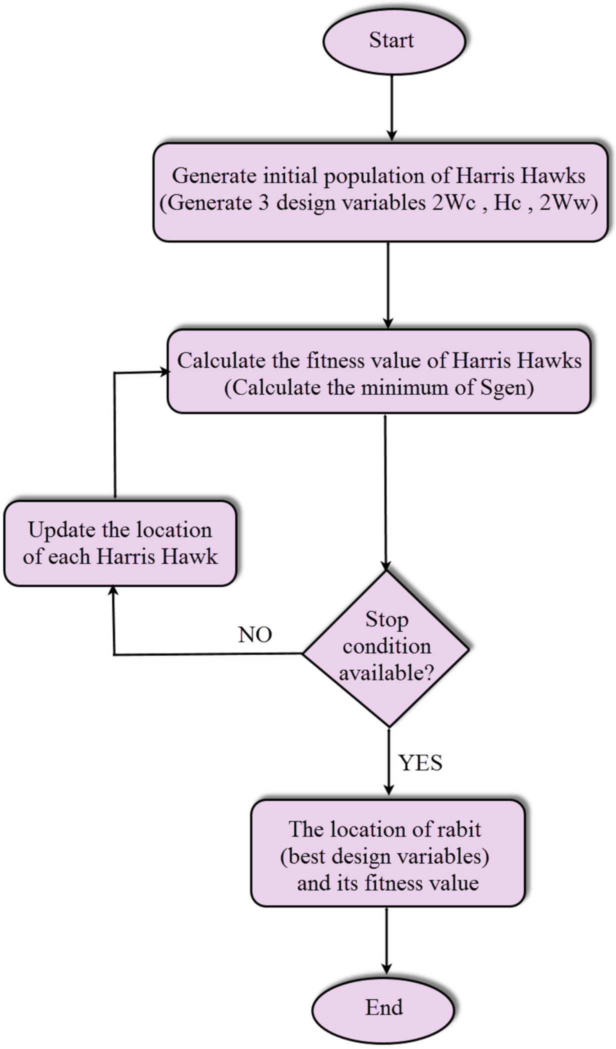
Start
Generate initial population of Harris Hawks
(Generate 3 design variables 2Wc , Hc , 2Ww)
Calculate the fitness value of Harris Hawks
(Calculate the minimum of Sgen)
Update the location of each Harris Hawk
NO
Stop condition available?
YES
The location of rabit (best design variables) and its fitness value
End

Fig. 3 HHO algorithm for the design of the microchannel heat sink

Table 1 Dimensions of heat sink and relevant material properties

Parameter	Value
Channel or heat sink length, L (mm)	51
Width of heat sink, W (mm)	51
Thermal conductivity of solid, k (at 300 K) (W $\mathrm{m^{-1}\,K^{-1}}$)	
Silicon	148
Cupper	401
Aluminium	237
Thermal conductivity of air, k_a at 300 K (Coolant) (W $\mathrm{m^{-1}\,K^{-1}}$)	
Air	0.0261
NH_3	0.0247
Density, ρ (kg $\mathrm{m^{-3}}$)	
Air	1.1614
NH_3	0.6894
Specific heat,c_p (J $\mathrm{kg^{-1}\,K^{-1}}$)	
Air	1007
NH_3	2158
Kinematic viscosity, ν ($\mathrm{m^2\,s^{-1}}$)	
Air	1.58×10^{-5}
NH_3	1.47×10^{-5}
Prandtl number, Pr	
Air	0.71
NH_3	0.89
Heat flux, q (W $\mathrm{cm^{-2}}$)	15
Ambient temperature, T_a (°C)	27
Tangential momentum accommodation coefficient, σ	0.85
Energy accommodation coefficient, σ_t	0.85

algorithms and are given in Table 1. We set maximum iteration number to 500 iterations to ensure the convergence. For further information on the PSO, GOA, WOA, DA, BeA algorithms, readers are referred to [3, 7–9, 54], respectively. All algorithms were simulated using Matlab (R2019a). Alternative materials to silicon and air are used to investigate their effect on the performance of microchannels. Computational efficiency of each algorithm is calculated as the average of 20 different runs and compared to each other. Model parameters and material properties of MCHS are given in Table 1.

4.1 Calibration of optimization parameters

Calibration of the optimization parameters plays an important role in minimizing entropy generation problems using the aforementioned algorithms. Therefore, in this section, we describe how to tune these parameters for obtaining the best possible solution. For that purpose, silicon–air case (Si–Air) is used as a test case, where the properties of Si–air are shown in Table 1. In the tuning process, all of the optimization parameters (shown in Table 2) are considered and varied across their nominal values generating a design of experiment (DOE) matrix. The optimization is run for all the elements of the DOE matrix and the optimization parameters corresponding to the minimum entropy generation are considered as the tuned parameters.

5 Results and discussions

Results are presented in two sections. In Sect. 1, HHO, GOA, WOA, DA optimization methods are used to minimize the entropy generation for optimizing the silicon microchannel design with air coolant fluid at various volume flow rate and Knudsen numbers. The results of this

Table 2 The optimization parameters

Optimization Method	Parameter	Value
GOA	Attraction length scale	1.4
	intensity of attraction	0.4
	search agent number	30
	Number of iteration	500
WOA	Search agent	30
	b	1
	Number of iteration	500
DA	Number of search agent	35
	Beta	1.5
	Number of iteration	500
HHO	Number of search agents	50
	β	1.5
	Number of iteration	500
PSO	Topology fully connected inertia factor	0.3
	C1	1
	C2	1
	Number of population	50
	Number of iteration	500
BeA	nScoutBee	50
	nSelectedSite	0.5*nScoutBe
	nEliteSite	0.4*nSelectedSite
	nSelectedSiteBee	0.5*nScoutBee
	nEliteSiteBee	0.5*nScoutBee
	Neighborhood radius damp rate	0.5
	Number of iteration	500

study are compared with those obtained from the previous studies conducted by Khan, Newton–Raphson and GA methods [48, 49]. The results from the optimization study indicate the effectiveness of the HHO algorithm based on the lower entropy generation results compared to other algorithms. In Sect. 2, a variety of materials with different thermal conductivity and coolant fluids are evaluated to obtain the optimum microchannel design. The results from this study are compared with six optimization algorithms: (HHO, GOA, WOA, DA, BeA, PSO).

5.1 Design using silicon–air

In this section, the entropy generation is minimized by HHO, GOA, WOA and DA optimization for silicon microchannel with air coolant at different flow rates and Knudsen numbers. The results of the comparison with Khan's previous works [48, 49] are summarized in Table 3. It is observed that by reducing the Knudsen number, the entropy generation increases. It should be mentioned that in Table 3, G is the volume flow rate of coolant and Kn is the Knudsen number, which were described in Sect. 2.2. The results indicate that the design from HHO algorithm is more efficient than others in the shortest time in a few iterations since the entropy generation is reduced as well as α_{c} and β. Using HHO algorithm, the entropy generation has been reduced by 63.31% compared to analytical NR method and 30.77% compared to GA algorithm from the literature. HHO has several characteristics that make it possible to show superior performance in exploring and exploiting in the search space. For example, the energy parameter, described in Sect. 3, improves the exploitation and exploration phase. HHO uses various array of diversification mechanism depending on the average location of hawks. The algorithm has different LF-based patterns with short length jumps, which would lead to increasing the capability of exploiting and exploring phases in HHO algorithm. Furthermore, search agents are able to improve their location by using progressive selection scheme in the algorithm. One of the superiority of HHO algorithm compared to previous algorithms is its capability to solve constrained problems and it can maintain its balance between exploitation and exploration. Moreover, HHO algorithm can use different search strategies based on r, E and jump (J) parameters, which allows HHO to balance the exploitation and exploration phases. The convergence curve for HHO, GOA, WOA, DA is shown in Fig. 4 for the various arrays of Kn and G. It is concluded from the convergence curve that, GOA, WOA and DA algorithms converge in 150 iterations. On the other hand, HHO algorithm as explained in Sect. 3 yields better results compared to other metaheuristic algorithms. As can be detected from Table 3, WOA is the second best algorithm after HHO (best results in Table 3 are highlighted as bold). The results show that minimum entropy generation [$S_{\mathrm{gen}} = 0.1268$ (W K^{-1})] is achieved for $G = 0.007$ m s^{-3} and Kn = 0.1 for silicon MCHSs with air as a coolant.

Figure 5 shows the variations of the entropy generation as a function of the volume flow rate for different Kn values. This figure is plotted for the specific design variables, (H_{c} as height of channel, $2w_{\mathrm{c}}$ as width of the channel, and $2w_{\mathrm{w}}$ as width of the fin), it can be observed that S_{gen} depends on these dimensions. Then, the parameters, which minimize S_{gen}, can be identified.

For some flow rate values, the entropy generation is decreasing while for others it is increasing. It is also deduced from the diagram that for each model there is a volume of volumetric flow rate in which the entropy generation is minimized. Different flow rate designs and microchannel materials can change this specific volume of flow rate. In Fig. 6, conductivity thermal changes induce significant changes in entropy generation. At a large Knudsen number, by increasing thermal conductivity, the entropy generation is reduced. Conductivity is a critical parameter on the microchannel design. It is known that a material with high conductivity in the design of microchannel improves the efficiency of the

Table 3 Comparison of optimum design variables and performance metrics

Indicator		α_c						β					
G (m^3 s^{-1})	Kn	NR Method [49]	GA OPT [48]	Current work				NR Method [49]	GA OPT [48]	Current work			
				GOA	WOA	DA	HHO			GOA	WOA	DA	HHO
0.005	0.1	0.164	0.081	0.018	0.012	0.015	0.0133	3.06	2.69	1.00	1	1.04	1.0469
	0.01	0.172	0.086	0.016	0.014	0.016	0.0132	3.13	3.05	1.10	1	1.17	1.0615
	0.001	0.175	0.091	0.015	0.015	0.020	0.0137	3.16	3.11	1.09	1	1.17	1.0914
0.007	0.1	0.194	0.097	0.016	0.015	0.016	0.0129	4.99	3.91	1.12	1	1.19	1.0366
	0.01	0.203	0.104	0.018	0.018	0.014	0.0163	5.16	5.20	1.31	1	1.18	1.3098
	0.001	0.207	0.112	0.022	0.019	0.019	0.0158	5.20	5.27	1.41	1	1.36	1.2685
0.009	0.1	0.222	0.119	0.018	0.017	0.017	0.0155	7.31	4.75	1.29	1	1.25	1.2450
	0.01	0.233	0.130	0.024	0.022	0.023	0.0187	7.59	6.20	1.59	1	1.63	1.5025
	0.001	0.237	0.136	0.024	0.023	0.022	0.0195	7.67	7.04	1.66	1	1.67	1.5654

Indicator		S_{gen}(W K^{-1})					
G (m^{3-1})	Kn	NR Method [49]	GA OPT [48]	Current work			
				GOA	WOA	DA	HHO
0.005	0.1	0.463	0.267	0.1463	0.1400	0.1395	**0.1362**
	0.01	0.511	0.288	0.1651	0.1620	0.1631	**0.1572**
	0.001	0.521	0.293	0.1692	0.1681	0.1814	**0.1633**
0.007	0.1	0.398	0.222	0.1356	0.1311	0.1327	**0.1268**
	0.01	0.462	0.250	0.1641	0.1617	0.1606	**0.1583**
	0.001	0.476	0.257	0.1788	0.1678	0.1718	**0.1657**
0.009	0.1	0.370	0.202	0.1405	0.1349	0.1390	**0.1313**
	0.01	0.451	0.241	0.1776	0.1708	0.1739	**0.1648**
	0.001	0.468	0.248	0.1830	0.1790	0.1778	**0.1717**

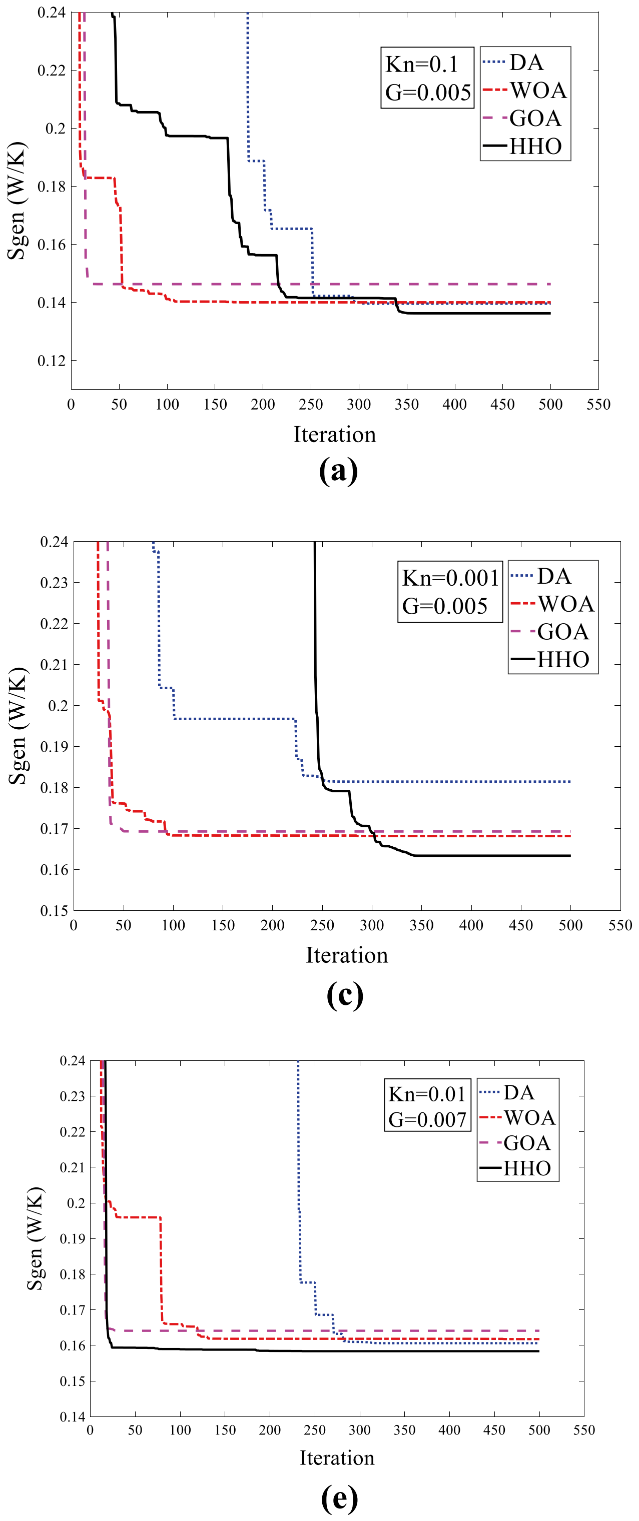

Fig. 4 S_{gen} versus iterations in 500 iterations for S–Air configuration corresponding to different G and Kn values

system considerably. The results of Figs. 5 and 6 are in line with Khan's findings from [47]. Our results show that there is a similar trend for S_{gen} versus volume flow rate between S_{gen} versus thermal conductivity as in the literature. This proves the accuracy of our formulation and numeric results.

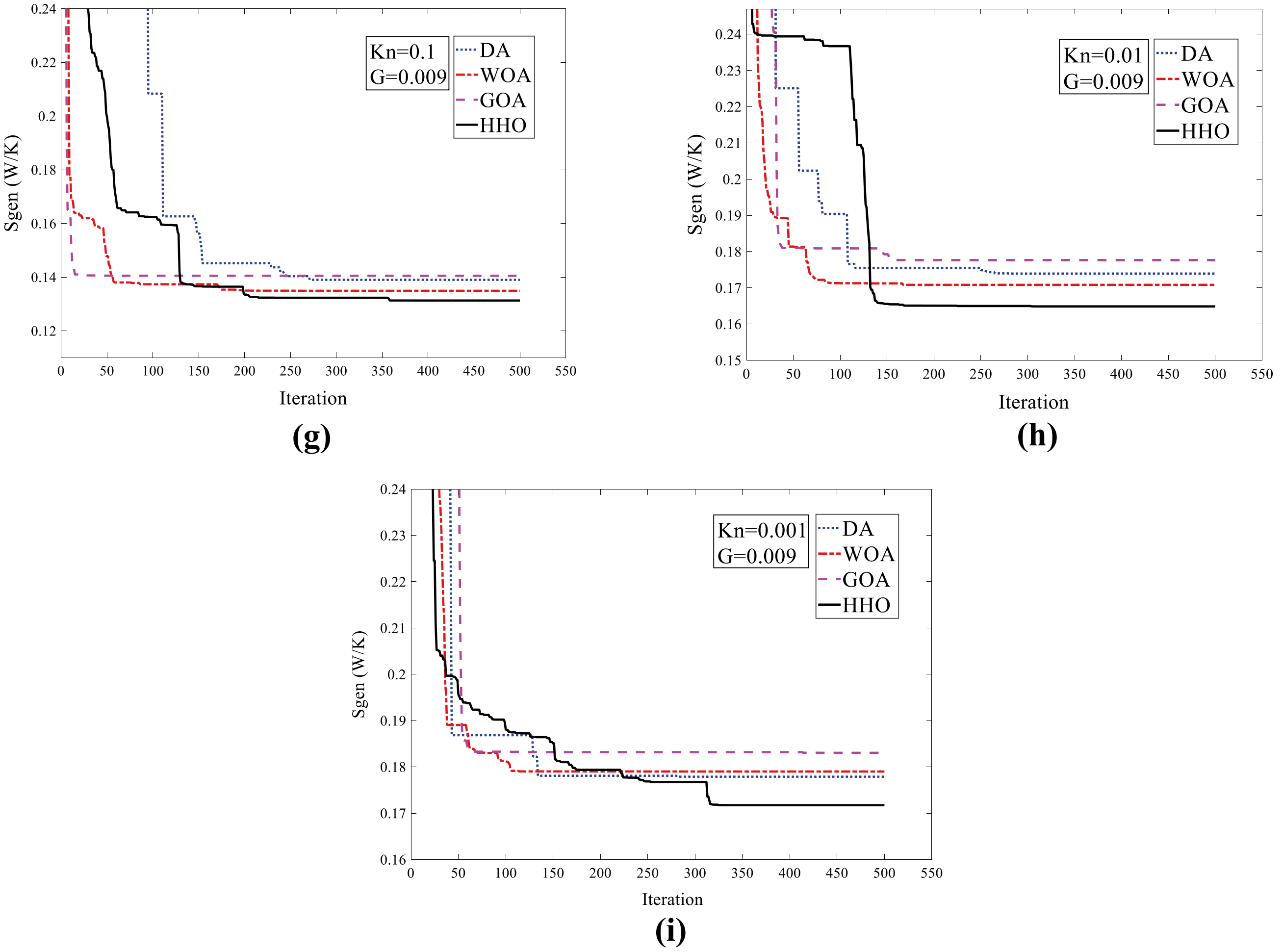

Fig. 4 (continued)

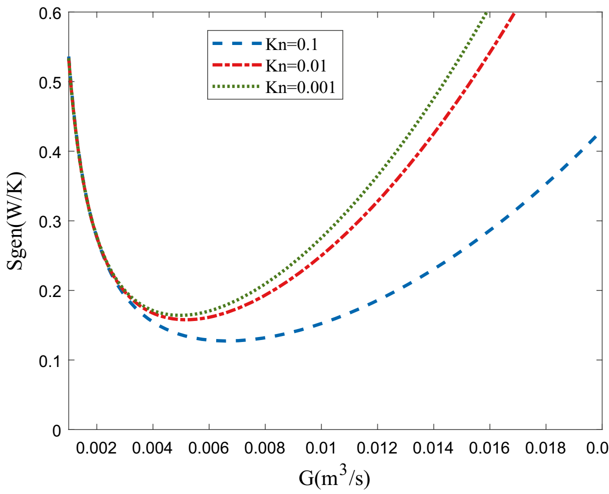

Fig. 5 The effect of volume flow rate on S_{gen} for various Kn

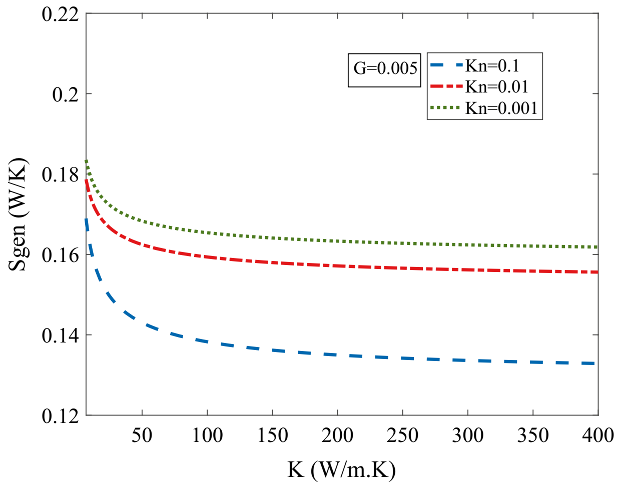

Fig. 6 The effect of thermal conductivity on S_{gen} for various Kn with $G = 0.005$

Table 4 Optimum design results from the application of optimization algorithms for different MCHSs

S_{gen} (W K^{-1})	Kn = 0.1						Kn = 0.01					
G (m^3 s^{-1})	PSO	BeA	DA	WOA	GOA	HHO	PSO	BeA	DA	WOA	GOA	HHO
Cu–NH$_3$												
0.005	0.1139	0.1039	0.1263	0.1239	0.1052	**0.0973**	0.1315	0.1165	0.1426	0.1222	0.1352	**0.1107**
0.006	0.1110	0.0942	0.1146	0.0981	0.1038	**0.0909**	0.1259	0.1118	0.1299	0.1125	0.1306	**0.1093**
0.007	0.1086	0.0904	0.1118	0.0937	0.0979	**0.0877**	0.1281	0.1136	0.1213	0.1177	0.1302	**0.1094**
0.008	0.1107	0.0920	0.1164	0.0903	0.1013	**0.0882**	0.1305	0.1176	0.1246	0.1142	0.1338	**0.1105**
0.009	0.1137	0.0932	0.1221	0.0922	0.1056	**0.0897**	0.1341	0.1195	0.1381	0.1150	0.1404	**0.1123**
Al–NH$_3$												
0.005	0.1222	0.1016	0.1164	0.1094	0.1333	**0.0990**	0.1443	0.1195	0.1226	0.1233	0.1311	**0.1126**
0.006	0.1198	0.0941	0.1113	0.1032	0.1281	**0.0920**	0.1408	0.1176	0.1184	0.1211	0.1291	**0.1104**
0.007	0.1176	0.0928	0.1095	0.1001	0.1133	**0.0891**	0.1419	0.1180	0.1180	0.1196	0.1222	**0.1110**
0.008	0.1202	0.0951	0.1106	0.1063	0.1241	**0.0899**	0.1466	0.1202	0.1261	0.1263	0.1236	**0.1122**
0.009	0.1211	0.0997	0.1139	0.1101	0.1283	**0.0912**	0.1483	0.1226	0.1328	0.1321	0.1308	**0.1143**
Si–NH$_3$												
0.005	0.1326	0.1063	0.1231	0.1073	0.1320	**0.1004**	0.1421	0.1247	0.1436	0.1426	0.1285	**0.1136**
0.006	0.1300	0.1004	0.1185	0.1053	0.1271	**0.0931**	0.1409	0.1226	0.1400	0.1321	0.1274	**0.1117**
0.007	0.1289	0.0999	0.1109	0.1038	0.1182	**0.0909**	0.1421	0.1242	0.1381	0.1273	0.1255	**0.1125**
0.008	0.1300	0.1002	0.1166	0.1086	0.1233	**0.0916**	0.1437	0.1249	0.1384	0.1314	0.1279	**0.1144**
0.009	0.1316	0.1089	0.1212	0.1141	0.1293	**0.0933**	0.1458	0.1263	0.1411	0.1364	0.1325	**0.1167**
CPU time (s)	1.1	1.7	10.36	0.46	1.31	0.25	1.1	1.7	10.36	0.46	1.31	0.25
Al–Air												
0.005	0.1561	0.1381	0.1476	0.1516	0.1500	**0.1310**	0.1911	0.1647	0.1741	0.1754	0.1903	**0.1565**
0.006	0.1548	0.1332	0.1455	0.1463	0.1477	**0.1249**	0.1888	0.1623	0.1725	0.1731	0.1851	**0.1551**
0.007	0.1538	0.1320	0.1423	0.1391	0.1423	**0.1248**	0.1905	0.1644	0.1719	0.1706	0.1811	**0.1563**
0.008	0.1562	0.1377	0.1444	0.1429	0.1436	**0.1264**	0.1936	0.1665	0.1752	0.1784	0.1823	**0.1586**
0.009	0.1579	0.1395	0.1511	0.1487	0.1455	**0.1286**	0.1989	0.1703	0.1801	0.1827	0.1849	**0.1618**
Cu–Air												
0.005	0.1541	0.1375	0.1486	0.1509	0.1456	**0.1298**	0.1936	0.1649	0.1875	0.1759	0.1873	**0.1546**
0.006	0.1493	0.1309	0.1436	0.1459	0.1441	**0.1234**	0.1900	0.1636	0.1831	0.1727	0.1832	**0.1537**
0.007	0.1514	0.1316	0.1381	0.1422	0.1388	**0.1236**	0.1923	0.1658	0.1829	0.1721	0.1769	**0.1549**
0.008	0.1556	0.1335	0.1441	0.1434	0.1409	**0.1244**	0.1940	0.1689	0.1842	0.1749	0.1811	**0.1565**
0.009	0.1577	0.1365	0.1477	0.1487	0.1451	**0.1264**	0.1954	0.1712	0.1863	0.1788	0.1853	**0.1593**
CPU Time (s)	1.1	1.7	10.36	0.46	1.31	0.25	1.1	1.7	10.36	0.46	1.31	0.25

S_{gen} (W K^{-1})	Kn = 0.001					
G (m^3 s^{-1})	PSO	BeA	DA	WOA	GOA	HHO
Cu–NH$_3$						
0.005	0.1430	0.1239	0.1368	0.1282	0.1491	**0.1154**
0.006	0.1398	0.1200	0.1321	0.1210	0.1414	**0.1147**
0.007	0.1388	0.1190	0.1324	0.1206	0.1359	**0.1139**
0.008	0.1422	0.1206	0.1339	0.1259	0.1452	**0.1154**
0.009	0.1446	0.1218	0.1425	0.1281	0.1537	**0.1175**
Al–NH$_3$						
0.005	0.1415	0.1242	0.1327	0.1258	0.1267	**0.1158**
0.006	0.1381	0.1204	0.1319	0.1243	0.1261	**0.1147**
0.007	0.1398	0.1225	0.1302	0.1237	0.1222	**0.1156**
0.008	0.1405	0.1241	0.1309	0.1319	0.1234	**0.1169**
0.009	0.1424	0.1269	0.1355	0.1366	0.1301	**0.1192**
Si–NH$_3$						

Table 4 (continued)

S_{gen} (W K^{-1}) G (m^3 s^{-1})	Kn = 0.001 PSO	 BeA	 DA	 WOA	 GOA	 HHO
0.005	0.1512	0.1253	0.1378	0.1329	0.1422	**0.1167**
0.006	0.1486	0.1232	0.1370	0.1317	0.1388	**0.1162**
0.007	0.1508	0.1267	0.1314	0.1286	0.1311	**0.1171**
0.008	0.1528	0.1274	0.1355	0.1321	0.1321	**0.1190**
0.009	0.1544	0.1311	0.1403	0.1383	0.1364	**0.1216**
CPU time (s)	1.1	1.7	10.36	0.46	1.31	0.25
Al–Air						
0.005	0.1936	0.1728	0.1839	0.1864	0.1739	**0.1617**
0.006	0.1910	0.1701	0.1817	0.1834	0.1721	**0.1613**
0.007	0.1941	0.1723	0.1794	0.1788	0.1688	**0.1627**
0.008	0.1972	0.1749	0.1821	0.1819	0.1744	**0.1663**
0.009	0.1988	0.1774	0.1874	0.1841	0.1767	**0.1686**
Cu–Air						
0.005	0.1932	0.1733	0.1813	0.1794	0.1804	**0.1606**
0.006	0.1901	0.1719	0.1791	0.1776	0.1789	**0.1599**
0.007	0.1920	0.1725	0.1785	0.1769	0.1773	**0.1609**
0.008	0.1939	0.1753	0.1811	0.1784	0.1801	**0.1632**
0.009	0.1953	0.1768	0.1819	0.1806	0.1826	**0.1661**
CPU time (s)	1.1	1.7	10.36	0.46	1.31	0.25

5.2 Design using alternative materials

In the second part, for better investigation six optimization algorithm (HHO, GOA, WOA, DA, BeA, PSO) are used to minimize the entropy generation. As it is mentioned in the previous section microchannel's conductivity has a significant effect on entropy generation of system. In this regard, three microchannels of copper and aluminum–silicon with two fluids of air and ammonia gas are investigated. Another important design consideration on the MCSH design is the coolant fluid. In this study, we consider two types of coolants: ammonia and air. Ammonia gas (R-717) is used extensively in industrial systems due to its known advantages. Firstly, ammonia is environmentally compatible. Second, ammonia has superior thermodynamic quality and requires less heat transfer area and hence uses less electricity. Moreover, the odor of ammonia makes it easy to detect the leaks. Finally, it is comparatively cheaper than other alternatives.

Six cases (1) Cu–NH_3:Cupper–ammonia, (2) Al–NH_3: (3) Aluminum–Ammonia, (4) Si–NH_3:silicon–ammonia, (5) Al–Air: Aluminum–Air, Cu–Air: Cupper–air and (6) Si–Air: silicon air) are evaluated with six algorithms to minimize the entropy generation (Si–Air was studied in Sect. 5.1).

Table 4 show the results for various Knudsen number and volumetric flow rates (best results in Table 4 are highlighted as bold). The results indicate the effectiveness and computational efficiency of the HHO method compared to other algorithms. In addition, its high search and exploration power is also visible in Fig. 7 for case Cu–NH_3. Considering the merits of HHO algorithm which are elaborated in the previous section, this algorithm is looking for optimal solutions by trying to balance the exploration and exploitation. The BeA algorithm found the solution in the same low number of iterations, and the higher iterations failed to produce better solutions but compare to other algorithms it shows superior performance. The opposite is seen in the HHO algorithm, which achieved better results in higher iterations by producing more acceptable solutions, indicating this novel algorithm's strength in examining problems. Another distinctive feature of this algorithm is conducting the optimization process in less time, which is recommended to use in more complex functions with more variables.

From Table 4 it can be concluded that material of microchannel and fluid as a coolant are effective parameters on entropy generation and the efficiency of system. Copper, compared to aluminum and silicon, has a higher conductivity and therefore leads to lower entropy generation. From the comparisons between Cu–NH_3 and Cu-air, entropy generation is reduced drastically for the Cu–NH_3 case, which is attributed to the use of ammonia as the coolant fluid.

Thermophysical properties, conductivity and specific heat capacity of ammonia can result in a better performance of microchannel's coolant fluid compare to air. In addition, using ammonia is advantageous as the leakage from a potential damage in the system would lead to early detection of

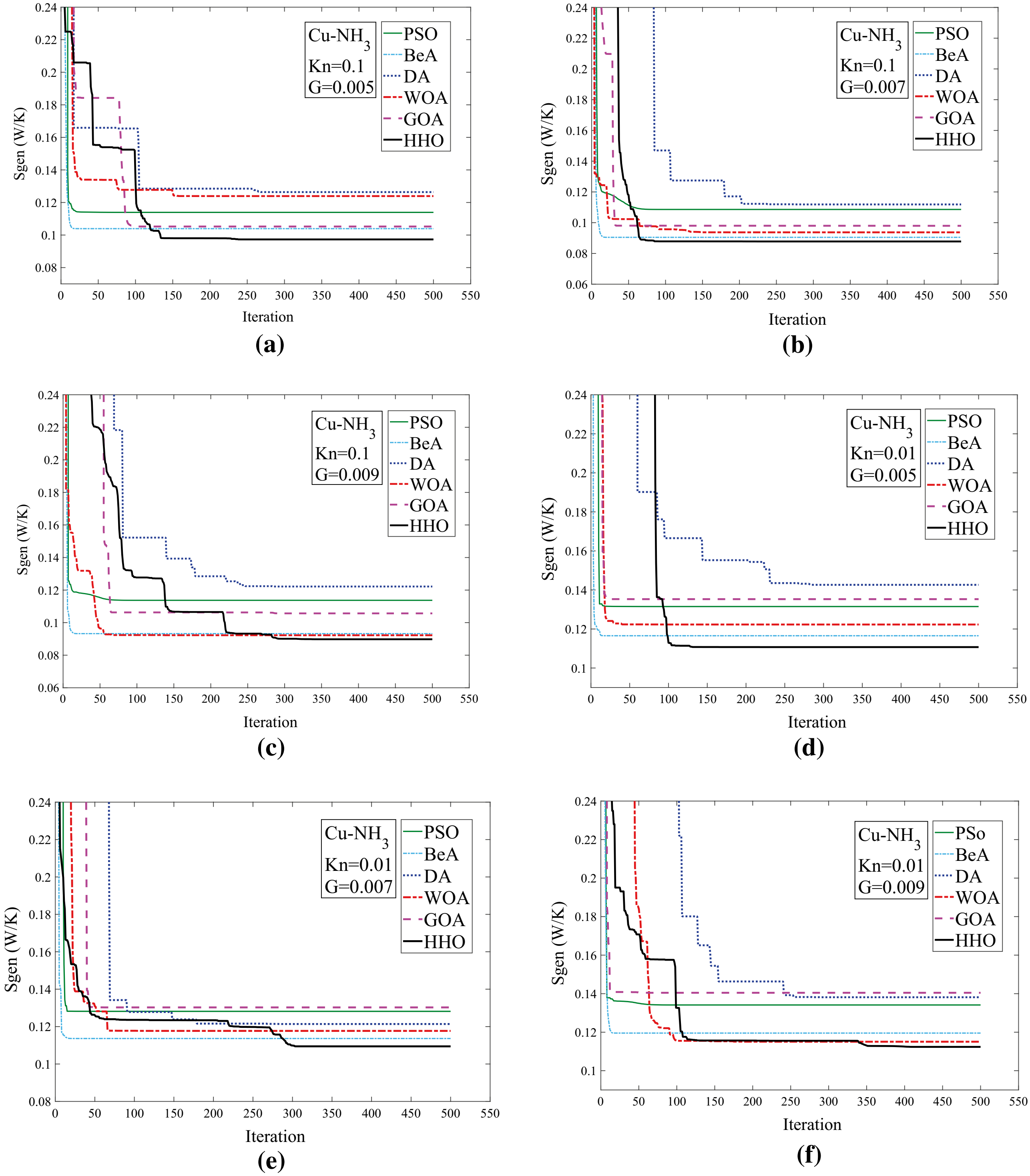

Fig. 7 Objective function versus iterations for Cu–NH$_3$ case for different *G* and Kn parameters from **a** to **i**

the damage due to its odor, which is not harmful to human health. Moreover, it has a lower density which makes it suitable for microscale applications.

It is fair to be mentioned that ammonia has some disadvantageous. The major disadvantage of ammonia as a coolant is its toxicity. Due to ammonia's hygroscopic nature, it migrates to moist areas of the body, including the eyes, nose, throat and moist skin and may cause severe burn injuries.

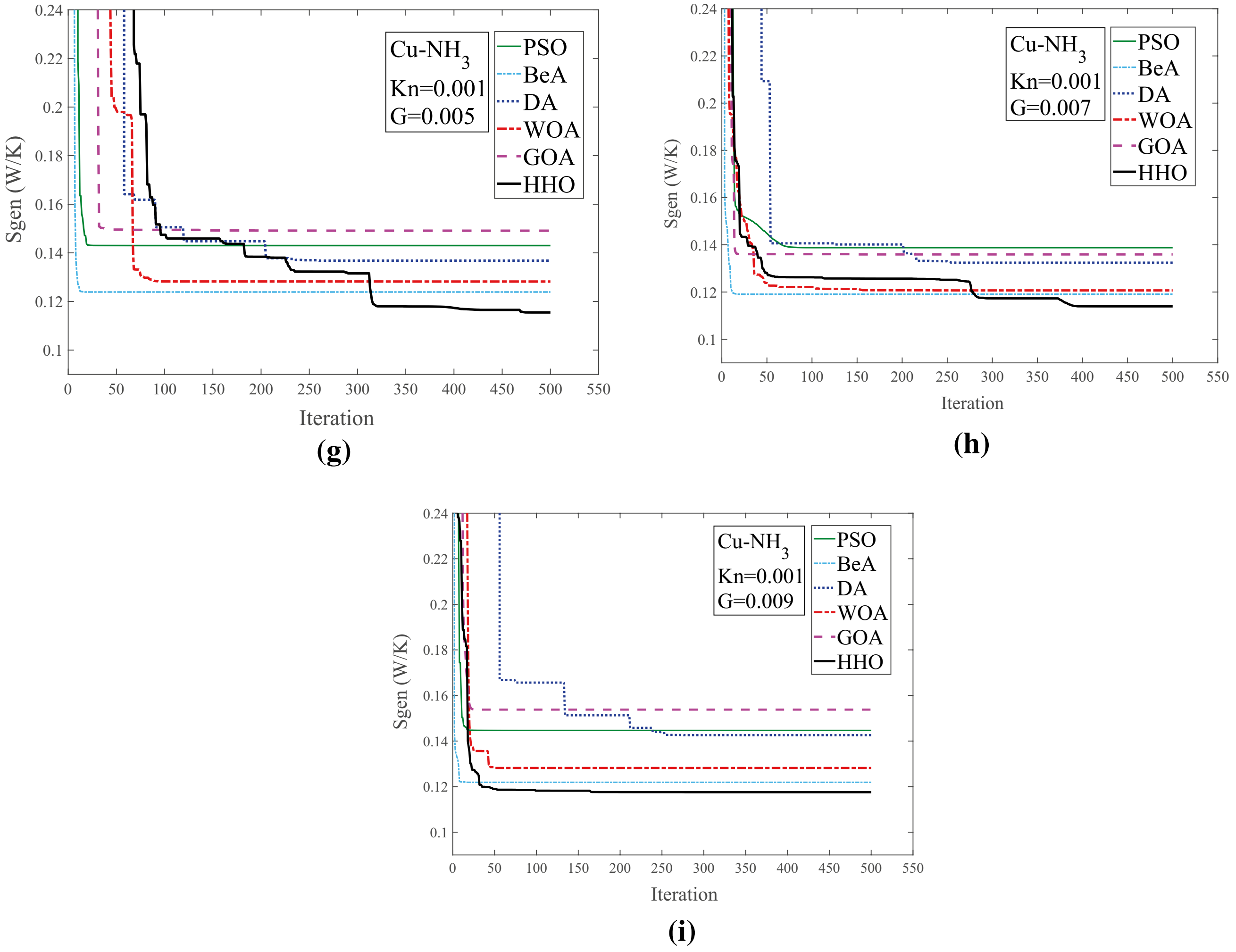

(g)

(h)

(i)

Fig. 7 (continued)

Figure 8 shows the minimum generation entropy data compared to the volumetric flow rate for the six design cases, indicating that the use of ammonium coolant performs better than using air as the coolant to minimize entropy generation as bad factor for system. This can be due to the high specific heat of ammonia compared to air.

As seen in the diagram, the best design is the copper-ammonia (Cu–NH$_3$), whose entropy generation value in volumetric flow rate 0.007 reaches its minimum value.

Even though ammonia has very attractive properties, it is a corrosive material when used with copper, brass and bronze. Therefore, we proposed to use aluminum-ammonia (Al-NH$_3$) in the microchannel design as Al–NH$_3$ is the second best case from the results of Fig. 8.

Reliability of aluminum has been proven as an efficient material in industry for many years. Advantageous of aluminum are summarized below:

- cost efficient and ductile
- good machinability
- toughness at subzero temperature
- suitable for soldering and welding
- cheaper than copper

6 Conclusion

In this paper, the effects of different channel aspect ratio, fin aspect ratio, heat sink materials and different Knudsen numbers in different flow rate have been studied. In this regard, the entropy generation is optimized with the powerful novel HHO method, which provides better results than previous works applying other methods and algorithms. The results obtained by the HHO method indicate that the entropy generation, which is a negative factor for the system, can be designed with a lower aspect ratio and fin aspect ratio, which in turn reduces the negative effect of this disturbing factor for the system.

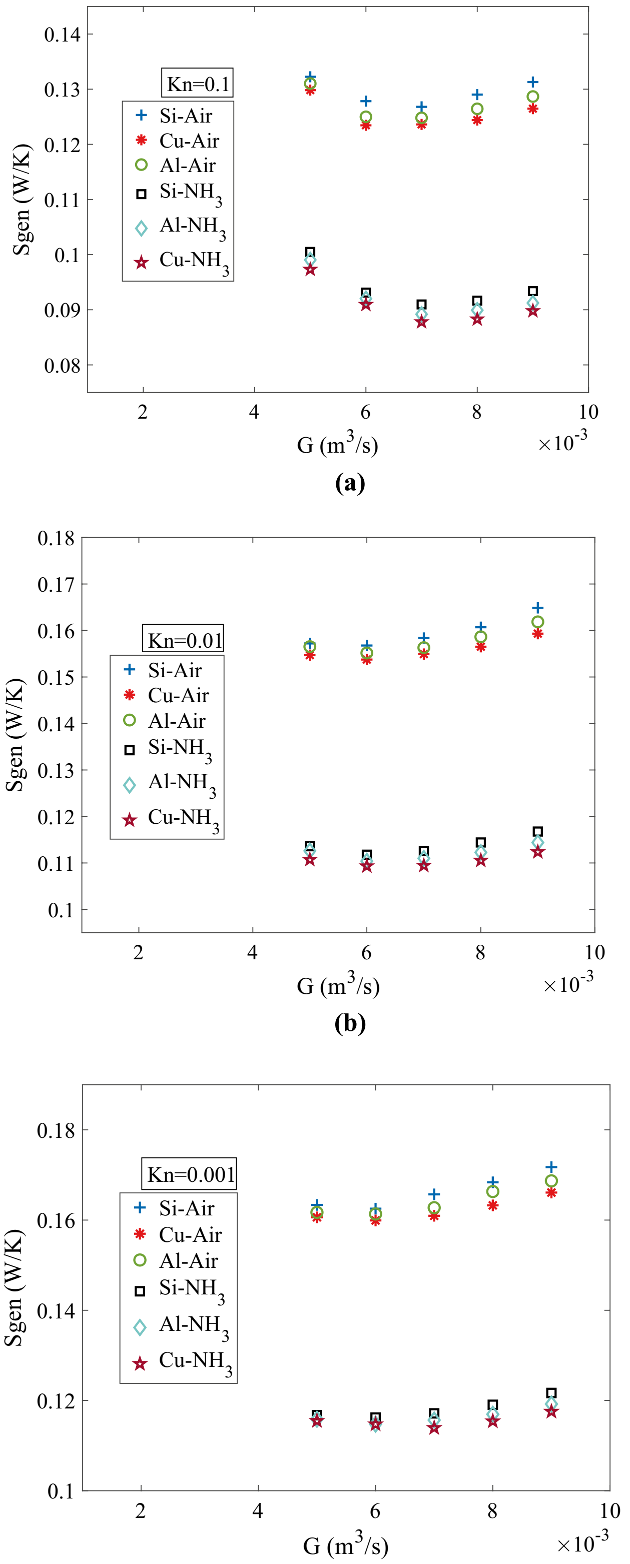

(a)

(b)

(c)

Fig. 8 Optimal S_{gen} versus G for different design of microchannel through **a**–**c**, for a various Kn

Alternative materials for the microchannel and coolant fluids were also assessed in terms of their effect on the performance of the system. Optimization results indicate that copper as the microchannel material and ammonia gas as the coolant results in the minimum entropy generation. Since ammonia is not resistive to corrosion, aluminum-ammonia (Al-NH3) is recommended as an alternative for microchannel material and coolant fluid.

In this paper, the newly introduced HHO optimization algorithm is used to minimize the entropy generation. This algorithm was compared to the five powerful algorithms of GOA, WOA, DA, BeA and PSA. It is found that the HHO algorithm yields a better solution than the well-known algorithms in less CPU time thanks to its strong exploration and search pattern. HHO has several characteristics that make it possible to finds solution based on stable equilibrium between diversification and intensification and it is able to converge towards global optimum without being trapped to local optimum solutions. This simulation results show that the application of this algorithm is a strong and efficient candidate in many engineering problems, which are modeled with complex functions and many variables.

It is well known that material parameters can effectively minimize the entropy generation (S_{gen}). other materials based on k_w, υ and ρ and etc. can be studied to improve the performance of MCHS design. Furthermore, it is possible to integrate HHO with other evolutionary schemes for improving the performance of HHO algorithm. These are acknowledged as future work.

References

1. Tuckerman DB, Pease RFW (1981) High-performance heat sinking for VLSI. IEEE Electron Device Lett 2(5):126–129
2. Li J, Peterson GP, Cheng P (2004) Three-dimensional analysis of heat transfer in a micro-heat sink with single phase flow. Int J Heat Mass Transf 47(19–20):4215–4231
3. Eberhart R, Kennedy J (1995) A new optimizer using particle swarm theory. In: MHS'95. Proceedings of the sixth international symposium on micro machine and human science. IEEE, pp 39–43
4. Atashpaz-Gargari E, Lucas C (2007) Imperialist competitive algorithm: an algorithm for optimization inspired by imperialistic competition. In: 2007 IEEE congress on evolutionary computation. IEEE¸pp 4661–4667
5. Dorigo M, Maniezzo V, Colorni A (1996) Ant system: optimization by a colony of cooperating agents. IEEE Trans Syst Man Cybern B Cybern 26(1):29–41
6. Karaboga D, Basturk B (2007) A powerful and efficient algorithm for numerical function optimization: artificial bee colony (ABC) algorithm. J Global Optim 39(3):459–471
7. Saremi S, Mirjalili S, Lewis A (2017) Grasshopper optimisation algorithm: theory and application. Adv Eng Softw 105:30–47
8. Mirjalili S, Lewis A (2016) The whale optimization algorithm. Adv Eng Softw 95:51–67

9. Mirjalili S (2016) Dragonfly algorithm: a new meta-heuristic optimization technique for solving single-objective, discrete, and multi-objective problems. Neural Comput Appl 27(4):1053–1073
10. Yildiz AR, Abderazek H, Mirjalili S (2019) A comparative study of recent non-traditional methods for mechanical design optimization. Arch Comput Methods Eng. https://doi.org/10.1007/s11831-019-09343-x
11. Moayedi H, Mu'azu MA, Kok Foong L (2019) Swarm-based analysis through social behavior of grey wolf optimization and genetic programming to predict friction capacity of driven piles. Eng Comput. https://doi.org/10.1007/s00366-019-00885-z
12. Moezi SA, Zakeri E, Zare A (2018) Structural single and multiple crack detection in cantilever beams using a hybrid Cuckoo-Nelder–Mead optimization method. Mech Syst Signal Process 99:805–831
13. Slowik A, Kwasnicka H (2017) Nature inspired methods and their industry applications—swarm intelligence algorithms. IEEE Trans Industr Inf 14(3):1004–1015
14. Li J, Lu J, Yao L, Cheng L, Qin H (2019) Wind–solar–hydro power optimal scheduling model based on multi-objective dragonfly algorithm. Energy Procedia 158:6217–6224
15. Suresh V, Sreejith S, Sudabattula SK, Kamboj VK (2019) Demand response-integrated economic dispatch incorporating renewable energy sources using ameliorated dragonfly algorithm. Electr Eng. https://doi.org/10.1007/s00202-019-00792-y
16. Abderazek H, Mirjalili AR, Yildiz S (2019) Comparison of recent optimization algorithms for design optimization of a cam-follower mechanism. Knowl Based Syst. https://doi.org/10.1016/j.knosys.2019.105237
17. Mirjalili S, Song Dong J (2020) Introduction to nature-inspired algorithms. In: Mirjalili S, Song Dong J, Lewis A (eds) Nature-inspired optimizers. Studies in computational intelligence, vol 811. Springer, Cham. https://doi.org/10.1007/978-3-030-12127-3_1
18. Heidari AA, Mirjalili S, Faris H, Aljarah I, Mafarja M, Chen H (2019) Harris hawks optimization: algorithm and applications. Future Gener Comput Syst 97:849–872
19. Moayedi H, Abdullahi MAM, Nguyen H, Rashid ASA (2019) Comparison of dragonfly algorithm and Harris hawks optimization evolutionary data mining techniques for the assessment of bearing capacity of footings over two-layer foundation soils. Eng Comput. https://doi.org/10.1007/s00366-019-00834-w
20. Moayedi H, Osouli A, Nguyen H, Rashid ASA (2019) A novel Harris hawks' optimization and k-fold cross-validation predicting slope stability. Eng Comput. https://doi.org/10.1007/s00366-019-00828-8
21. Aleem SHA, Zobaa AF, Balci ME, Ismael SM (2019) Harmonic overloading minimization of frequency-dependent components in harmonics polluted distribution systems using Harris hawks optimization algorithm. IEEE Access 7:100824–100837
22. Yildiz AR, Yildiz BS, Sait SM, Li X (2019) The Harris hawks, grasshopper and multi-verse optimization algorithms for the selection of optimal machining parameters in manufacturing operations. Mater Test 61(8):725–733
23. Golilarz NA, Addeh A, Gao H, Ali L, Roshandeh AM, Munir HM, Khan RU (2019) A new automatic method for control chart patterns recognition based on ConvNet and Harris Hawks meta heuristic optimization algorithm. IEEE Access 7:149398–149405
24. Mehta MS, Singh MB, Gagandeep M (2019) Harris Hawks optimization for solving optimum load dispatch problem in power system. Int J Eng Res Technol 8(6):962–968
25. Yildiz BS, Yildiz AR (2019) The Harris hawks optimization algorithm, salp swarm algorithm, grasshopper optimization algorithm and dragonfly algorithm for structural design optimization of vehicle components. Mater Test 61(8):744–748
26. Golilarz NA, Gao H, Demirel H (2019) Satellite image de-noising with Harris hawks meta heuristic optimization algorithm and improved adaptive generalized gaussian distribution threshold function. IEEE Access 7:57459–57468
27. Ekinci S, Hekimoğlu B, Demirören A, Kaya S (2019) Harris Hawks optimization approach for tuning of FOPID controller in DC–DC buck converter. In: 2019 International artificial intelligence and data processing symposium (IDAP). IEEE, pp 1–9
28. Too J, Abdullah AR, Mohd Saad N (2019) A new quadratic binary harris hawk optimization for feature selection. Electronics 8(10):1130
29. Hussain K, Zhu W, Salleh MNM (2019) Long-term memory Harris' hawk optimization for high dimensional and optimal power flow problems. IEEE Access 7:147596–147616
30. Chen H, Jiao S, Wang M, Heidari AA, Zhao X (2019) Parameters identification of photovoltaic cells and modules using diversification-enriched Harris hawks optimization with chaotic drifts. J Clean Prod. https://doi.org/10.1016/j.jclepro.2019.118778
31. Jia H, Lang C, Oliva D, Song W, Peng X (2019) Dynamic Harris hawks optimization with mutation mechanism for satellite image segmentation. Remote Sens 11(12):1421
32. Yildiz AR, Yildiz BS, Sait SM, Bureerat S, Pholdee N (2019) A new hybrid Harris hawks–Nelder–Mead optimization algorithm for solving design and manufacturing problems. Mater Test 61(8):735–743
33. Bao X, Jia H, Lang C (2019) A novel hybrid Harris hawks optimization for color image multilevel thresholding segmentation. IEEE Access 7:76529–76546
34. Bui DT, Moayedi H, Kalantar B, Osouli A, Pradhan B, Nguyen H, Rashid ASA (2019) A novel swarm intelligence—Harris hawks optimization for spatial assessment of landslide susceptibility. Sensors 19(16):3590
35. Wang ZH, Wang XD, Yan WM, Duan YY, Lee DJ, Xu JL (2011) Multi-parameters optimization for microchannel heat sink using inverse problem method. Int J Heat Mass Transf 54(13–14):2811–2819
36. Bello-Ochende T, Liebenberg L, Meyer JP (2007) Constructal cooling channels for micro-channel heat sinks. Int J Heat Mass Transf 50(21–22):4141–4150
37. Cruz-Duarte JM, Garcia-Perez A, Amaya-Contreras IM, Correa-Cely CR (2016) Designing a microchannel heat sink with colloidal coolants through the entropy generation minimisation criterion and global optimisation algorithms. Appl Therm Eng 100:1052–1062
38. Cruz J, Amaya I, Correa R (2015) Optimal rectangular microchannel design, using simulated annealing, unified particle swarm and spiral algorithms, in the presence of spreading resistance. Appl Therm Eng 84:126–137
39. Adham AM, Mohd-Ghazali N, Ahmad R (2014) Optimization of a rectangular microchannel heat sink using entropy generation minimization (EGM) and genetic algorithm (GA). Arabian Journal for Science and Engineering 39(10):7211–7222
40. Husain A, Kim KY (2009) Thermal optimization of a microchannel heat sink with trapezoidal cross section. J Electron Packag 131(2):021005
41. Husain A, Kim KY (2010) Enhanced multi-objective optimization of a microchannel heat sink through evolutionary algorithm coupled with multiple surrogate models. Appl Therm Eng 30(13):1683–1691
42. Mohd-Ghazali N, Jong-Taek O, Chien NB, Chi KI, Zolpakar NA, Ahmad R (2014) Multiobjective optimization of microchannels with experimental convective heat transfer coefficient of liquid ammonia. In: International conference on industrial, engineering and other applications of applied intelligent systems. Springer, Cham, pp 470–478

43. Xia GD, Jia YT, Li YF, Ma DD, Cai B (2016) Numerical simulation and multiobjective optimization of a microchannel heat sink with arc-shaped grooves and ribs. Numer Heat Transf Part A Appl 70(9):1041–1055
44. Hamadneh N, Khan W, Tilahun S (2018) Optimization of microchannel heat sinks using prey-predator algorithm and artificial neural networks. Machines 6(2):26
45. Singh BP, Garg H, Lall AK (2016) Optimization of microchannel heat sink using genetic algorithm and Taguchi method. In: AIP conference proceedings. AIP Publishing, vol 1724, no 1, p 020014
46. Deena R, Sai Sundara Krishnan GA (2019) A novel investigation of heat transfer characteristics in hybrid micro channel heat sink structure: opposition based ant lion optimization. Surf Rev Lett. https://doi.org/10.1142/S0218625X19501439
47. Khan WA, Kadri MB, Ali Q (2013) Optimization of microchannel heat sinks using genetic algorithm. Heat Transf Eng 34(4):279–287
48. Khan WA, Yovanovich MM, Culham J. R (2006) Optimization of microchannel heat sinks using entropy generation minimization method. In: Twenty-second annual ieee semiconductor thermal measurement and management symposium. IEEE, pp 78–86
49. Khan WA, Yovanovich MM (2008) Analytical modeling of fluid flow and heat transfer in microchannel/nanochannel heat sinks. J Thermophys Heat Transf 22(3):352–359
50. Incropera Frank P, DeWitt DP (1996) Fundamentals of heat and mass transfer, vol 4. Wiley, New York
51. Kleiner MB, Kuhn SA, Haberger K (1995) High performance forced air cooling scheme employing microchannel heat exchangers. IEEE Trans Compon Packag Manuf Technol Part A: 18(4):795–804
52. Kays WM, London AL (1964) Compact heat exchangers. McGraw Hill, New York
53. Yang XS (2010) Nature-inspired metaheuristic algorithms. Luniver press, Bar Harbor
54. Pham DT, Ghanbarzadeh A, Koç E, Otri S, Rahim S, Zaidi M (2006) The bees algorithm—a novel tool for complex optimization problems. In: Intelligent production machines and systems. Elsevier Science Ltd., pp 454–459

Publisher's Note Springer Nature remains neutral with regard to jurisdictional claims in published maps and institutional affiliations.